World Cancer Research Journal

WCRJ 2025; 12 : e2975
10.32113/wcrj_202512_2975

AKR7A2 PROMOTES HEPATOCELLULAR CARCINOMA PROGRESSION THROUGH AFFECTING TUMOR ASSOCIATED MACROPHAGE POLARIZATION AND OXIDATIVE PHOSPHORYLATION

H. CUI[1], Q.-Q. LONG[1], L. ZHANG[1], H. TIAN[1,2,3]

• • •

[1]Department of Pathology, The Affiliated Hospital of Youjiang Medical University for Nationalities, Baise, China
[2]The Key Laboratory of Molecular Pathology (Hepatobiliary Diseases) of Guangxi, Baise, China
[3]State Key Laboratory of Systems Medicine for Cancer, Shanghai Cancer Institute, Renji Hospital, Shanghai Jiao Tong University School of Medicine, Shanghai, China

Corresponding Author
Hua Tian, Ph.D., e-mail: htian@shsci.org

ABSTRACT – *Objective:* The aldo-keto reductase (AKR) superfamily catalyzes the NAD(P)H-dependent reduction of aldehydes to less reactive alcohols, playing a critical role in detoxification and cellular redox homeostasis. AKR family members have been increasingly implicated in tumor progression across various cancers. However, the functional role and mechanism of AKR7A2 in hepatocellular carcinoma (HCC) progression remain poorly understood. Here, we identified an essential role of AKR7A2 in HCC progression.

Materials and Methods: The expression of AKR7A2 was analyzed in HCC tissues and human cell line models via immunohistochemistry (IHC) and Western blotting. The influence of AKR7A2 on HCC proliferation, migration, and invasion was assessed through CCK-8, colony formation, and Transwell assays. Potential molecular mechanisms were explored through bioinformatics analysis of The Cancer Genome Atlas (TCGA) and Gene Expression Omnibus (GEO) databases.

Results: We found that AKR7A2 expression was upregulated and significantly associated with poor prognosis. Elevated AKR7A2 expression was also linked to resistance to radiotherapy and sorafenib treatment. Knockdown of AKR7A2 suppresses HCC cell proliferation, migration, and invasion. Bioinformatics analysis further demonstrated that expression of AKR7A2 was positively correlated with oxidative phosphorylation (OXPHOS), mitochondrial biogenesis, PPARG expression, and tumor-associated macrophage polarization.

Conclusions: Taken together, our results indicate that AKR7A2 promotes HCC cell proliferation, migration, and invasion through PPARG-mediated OXPHOS and tumor-associated macrophage polarization. Therefore, AKR7A2 represents a promising therapeutic target for the treatment of HCC.

KEYWORDS: AKR7A2, Oxidative phosphorylation, Tumor-associated macrophage polarization, Hepatocellular carcinoma, Progression.

INTRODUCTION

Hepatocellular carcinoma (HCC) is the sixth most common cancer worldwide and the third leading cause of cancer-related mortality[1,2]. The most significant contributing factor to the development of HCC is the chronic process of inflammation and remodeling of the cirrhotic liver, in which the interaction between the tumor microenvironment (TME) and cancer cells plays a pivotal role[3,4]. Surgical resection remains a cornerstone of curative treatment for patients with early-stage disease[5]. Despite significant advances in molecular targeted therapies and immunotherapy over the past decade, overall treatment outcomes for HCC

remain suboptimal[6-8]. The high rates of recurrence, intrinsic or acquired resistance to systemic therapies, and profound tumor heterogeneity continue to pose major clinical challenges[9]. Therefore, a deeper understanding of the oncogenic signaling pathways and immune regulatory mechanisms that drive HCC progression is crucial for developing more effective therapeutic strategies and improving patient prognosis.

The aldo-keto reductase (AKR) superfamily comprises enzymes that catalyze the NAD(P)H-dependent reduction of reactive aldehydes and ketones to less reactive alcohols, playing key roles in detoxification, lipid metabolism, and steroid hormone biosynthesis[10]. In eukaryotes, AKR enzymes are classified into 15 families (AKR1-AKR15) based on sequence homology. Humans express 15 functional AKR isoforms, including AKR1A1, AKR1B1, AKR1B10, AKR1B15, AKR1C1-C4, AKR1D1, AKR1E2, AKR6A3, AKR6A5, AKR6A9, AKR7A2, and AKR7A3[11]. We have previously demonstrated that AKR1C3 was markedly upregulated in HCC and correlates with poor patient prognosis[12]. Furthermore, AKR1C3 confers ferroptosis resistance in HCC by modulating the YAP/SLC7A11 signaling axis[13].

AKR7A2, a member of the AKR superfamily, is predominantly expressed in metabolically active tissues such as the liver and kidney. It exhibits catalytic activity toward reactive aldehydes generated during lipid peroxidation, thereby playing a critical role in cellular defense against oxidative stress by mitigating ROS-induced damage[14,15]. Through the detoxification of cytotoxic aldehydes and interactions with stress-responsive proteins such as cytoglobin, AKR7A2 contributes to redox homeostasis and cellular protection[16]. While these functions suggest a potential role in cancer biology, the involvement of AKR7A2 in HCC progression remains poorly understood. In this study, we investigate the functional role of AKR7A2 in HCC and elucidate the underlying molecular mechanisms.

MATERIALS AND METHODS

Cell lines and cell culture

Huh7 cells were obtained from Riken Cell Bank (Tsukuba, Japan). HepG2 cell lines were purchased from the American Type Culture Collection (ATCC, Manassas, VA, USA). The MHCC-LM3 and MHCC-97H cell lines were obtained from the Liver Cancer Institute, Zhongshan Hospital of Fudan University (Shanghai, China). All HCC cell lines used were cultured in Dulbecco's Modified Eagle's Medium (DMEM) (Gibco, Thermo Fisher Scientific Inc., Waltham, MA, USA) supplemented with 10% heat-inactivated fetal bovine serum (Gibco) and maintained at 37°C in a humidified incubator with 5% CO_2. All of the cell lines were authenticated and characterized by the suppliers. Cells were used within 6 months of resuscitation. These cell lines were mycoplasma-free and routinely authenticated by quality examinations of morphology and growth profile.

Western Blotting

Total protein was extracted using a RIPA lysis buffer supplemented with Protease and phosphatase inhibitor cocktail. The protein concentrations were quantified using the BCA Protein Assay Kit in accordance with the manufacturer's instructions[17]. Total cellular proteins were separated by SDS-polyacrylamide gel electrophoresis (SDS-PAGE) and transferred onto polyvinylidene difluoride (PVDF) membranes (Millipore (Merck KGaA, Darmstadt, Germany). Membranes were blocked with 5% non-fat milk or bovine serum albumin (BSA) in Tris-buffered saline containing 0.1% Tween-20 (TBST) for 1 h at room temperature, then incubated overnight at 4°C with primary antibodies diluted in blocking buffer. After three washes with TBST, membranes were incubated with horseradish peroxidase (HRP)-conjugated secondary antibodies for 1 h at room temperature. Immunoreactive bands were visualized using enhanced chemiluminescence (ECL) detection reagent (Pierce, Thermo Fisher Scientific, Rockford, IL, USA) and imaged on a chemiluminescent detection system. β-actin served as a loading control to confirm equal protein loading across samples.

Cell Proliferation and Colony Formation Assays

Cell proliferation was assessed using the Cell Counting Kit-8 (CCK-8) (Bimake, Houston, TX, USA) according to the manufacturer's instructions[18]. Briefly, cells were seeded in 96-well plates and allowed to adhere overnight. At the indicated time points, 10 µL of CCK-8 solution was added to each well,

and the plates were incubated at 37°C for 1-4 h. The absorbance at 450 nm was measured using a microplate reader. Each experiment was performed in triplicate and repeated independently at least three times.

Colony formation assays were conducted following previously described protocols[19]. HCC cells were seeded into 6-well plates at a density of 10^4 cells/well and incubated at 37°C for 2 weeks. Colonies were fixed with 4% phosphate-buffered formalin (pH 7.4) and subjected to Giemsa staining for 15 minutes. Each assay was performed in three separate experiments.

Wound-Healing Assay

Cell migration was evaluated using the wound healing (scratch) assay[20]. HCC cells were seeded into 6-well plates and cultured to 100% confluence to form a confluent monolayer. Wounds were created by scratching the monolayer with a sterile 10-µL pipette tip. After scratching, cell debris was removed by washing with phosphate-buffered saline (PBS), and fresh culture medium was added. Cells were then incubated at 37°C in a 5% CO_2 humidified incubator. Images of the wound areas were captured at 0-, 48-, and 72-hours post-scratching using an inverted light microscope. Wound closure was quantified by measuring the change in gap width over time using image analysis software (ImageJ).

Migration and Invasion Assays

Cell migration and invasion were assessed using Transwell assays according to established protocols[21]. For migration, cells were serum-starved overnight and then resuspended in serum-free DMEM. Cells were seeded into the upper chamber of a Transwell insert with an 8-µm pore size (Corning, NY, USA). For invasion assays, the upper chamber was pre-coated with Matrigel (BD Biosciences, NJ, USA) to mimic the extracellular matrix. The lower chamber contained DMEM supplemented with 10% FBS as a chemoattractant. After incubation for 24 h (migration) or 48 h (invasion) at 37°C in 5% CO_2, non-migrated or non-invaded cells on the upper surface of the membrane were gently removed with a cotton swab. Cells that had migrated or invaded the lower surface were fixed with 4% formalin, stained with Giemsa solution, and imaged under a light microscope. The number of migrated or invaded cells was quantified by counting the nuclei in five randomly selected fields of view per insert. Each experiment was performed in triplicate and repeated independently at least three times

Immunohistochemistry (IHC)

IHC assays were conducted as reported previously[22]. A total of 95 HCC tissues were obtained from the Affiliated Hospital of Youjiang Medical College for Nationalities. The clinicopathological features of HCC patients (n = 95) are shown in Table 1. Briefly, tissue sections were deparaffinized in xylene and rehydrated through a graded ethanol series to distilled water. Antigen retrieval was performed by heating sections in a microwave oven to just below boiling temperature using 10 mM sodium citrate buffer (pH 6.0) for 20 min. After cooling to room temperature, sections were washed three times with PBS. Endogenous peroxidase activity was blocked by incubating the sections with 3% hydrogen peroxide for 10 min at room temperature. Sections were then incubated overnight at 4°C with primary antibodies diluted in antibody diluent. Following three PBS washes, sections were incubated with horseradish peroxidase (HRP)-conjugated secondary antibody at 37°C for 30 min. Antigen detection was performed using a diaminobenzidine (DAB) chromogen solution, and nuclei were counterstained with Mayer's hematoxylin.

Statistical Analysis

All data are expressed as mean ± standard deviation (SDs). Comparisons between two groups were performed using the unpaired two-tailed Student's *t*-test. For comparisons among three groups, one-way analysis of variance (ANOVA) was used. Survival analyses were conducted using the Kaplan-Meier method, and differences in survival curves were assessed using the log-rank test. $p < 0.05$ was considered statistically significant.

Table 1. Clinicopathological features of HCC patients (95 cases).

Clinicopathological features	Number
Age	
<50	44
≥50	51
Gender	
Male	78
Female	16
Missing	1
Intrahepatic Metastasis	
Negative	86
Positive	9
Grade	
I	13
II -III	82
AFP (ng/mL)	
≤20	32
>20	56
Missing	7
HBV	
Negative	27
Positive	67
Missing	1
Vessel carcinoma embolus (VCE)	
Negative	90
Positive	5

RESULTS

Elevated AKR7A2 Expression Predicts Poor Prognosis in HCC

We first analyzed AKR7A2 expression using data from The Cancer Genome Atlas (TCGA). We found that AKR7A2 mRNA levels were significantly elevated in HCC tissues compared to adjacent noncancerous tissues (Figure 1A). In addition, AKR7A2 expression level was negatively correlated with radiotherapy and sorafenib response using TCGA data and GEO data (Figure 1B-1C). We next investigated the association between AKR7A2 expression and patient prognosis. Kaplan-Meier survival analysis revealed that patients with high AKR7A2 expression had significantly shorter overall survival (OS) compared to those with low expression (Figure 1D).

We next evaluated AKR7A2 expression in HCC tissues by IHC. Based on IHC staining intensity and extent, patients were stratified into high or low AKR7A2 expression groups (Figure 1E). High AKR7A2 expression was significantly associated with the presence of microvascular invasion (MVI, also referred to as vessel carcinoma embolus, VCE) and hepatitis B virus (HBV) positivity (Table 2). However, no significant correlation was observed between AKR7A2 expression and other clinicopathological parameters, including age, sex, serum alpha-fetoprotein (AFP) level, or intrahepatic metastasis (Table 2). Taken together, these findings indicate that high AKR7A2 expression is associated with a poor prognosis in HCC patients and that AKR7A2 may play an important role in promoting the malignant progression of HCC.

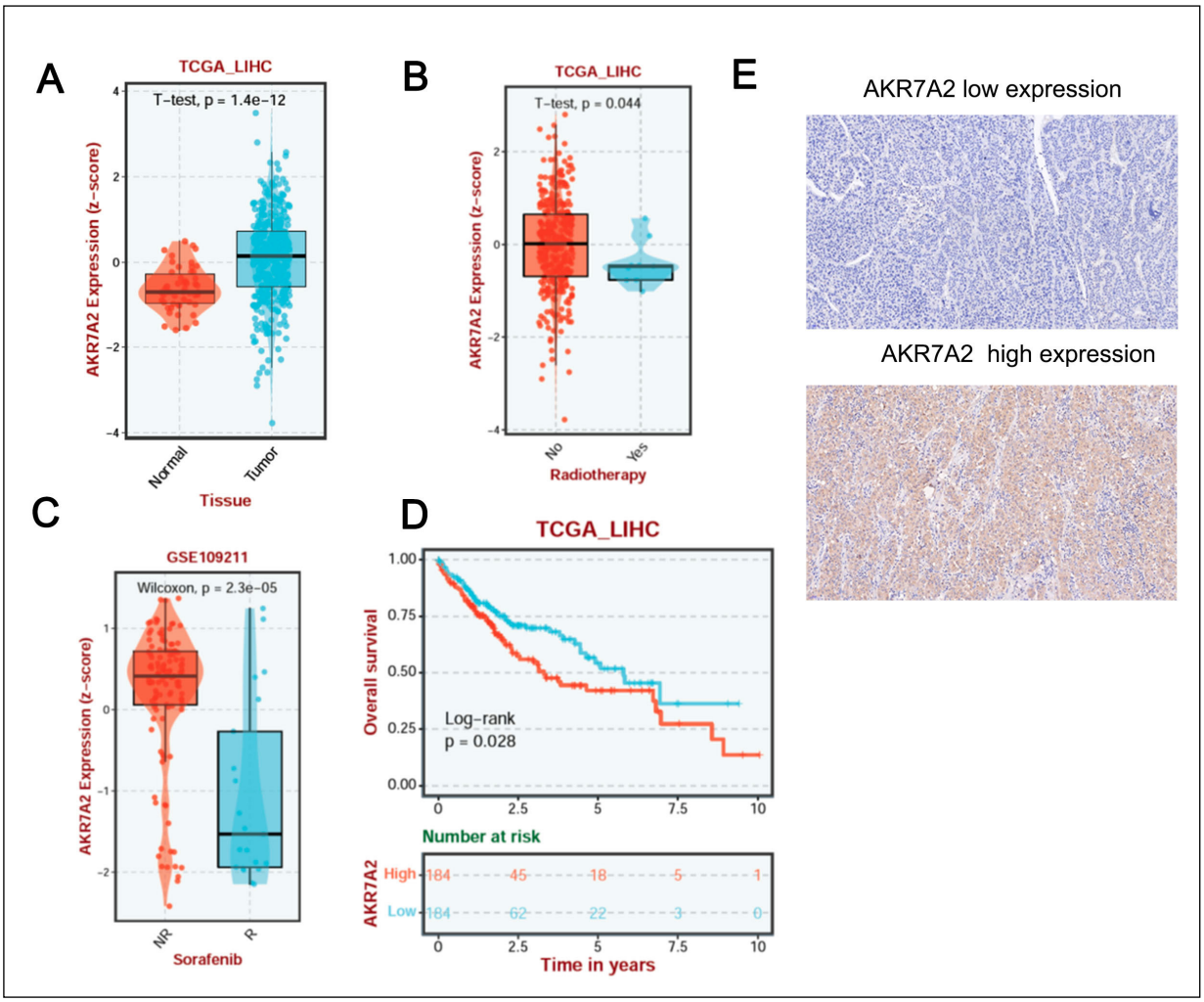

Figure 1. Overexpression of AKR7A2 is associated with a poor prognosis in HCC patients. *A*, The expression of AKR7A2 in HCC tissues was compared with that in the corresponding noncancerous liver tissues in the TCGA datasets. *B*, The expression of AKR7A2 in HCC patients with radiotherapy response or no-response in the TCGA datasets. *C*, The expression of AKR7A2 in HCC patients with sorafenib response or no-response in the GSE109211 datasets. *D*, Overall survival analysis of HCC patients TCGA cohort stratified by the AKR7A2 expression. *E*, The expression of AKR7A2 in HCC tissues using IHC.

AKR7A2 Promotes HCC Cell Proliferation

To verify the function of AKR7A2 in HCC, we first examined the expression of AKR7A2 in HCC cell lines. The MHCC-LM3 and HepG2 cells were selected for loss-of-function studies due to their high endogenous AKR7A2 levels (Figure 2A-2B). A stable knockdown cell line of AKR7A2 was established using lentiviral transduction (Figure 2C-2D). We found that AKR7A2 knockdown inhibited HCC cell proliferation and decreased the colony formation ability (Figure 2E-2F).

AKR7A2 Promotes HCC Cell Migration and Invasion

Since AKR7A2 was shown to be related to vessel carcinoma embolus (Table 2), we further examined the effect of AKR7A2 on the migration and invasion of HCC cells. We found that the silencing of AKR7A2 mitigated cell migration using the Wound-healing assay (Figure 2G). Furthermore, Transwell assay showed that silencing AKR7A2 mitigated cell migration and invasion (Figure 2H).

Table 2. Correlation between AKR7A2 levels in HCC patients and their clinicopathological characteristics.

Clinicopathological features	Number	Low expression N (%)	High expression N (%)	*p*-value
Age				
<50	44	28(50.0)	16(41.0)	0.388
≥50	51	28(50.0)	23(59.0)	
Gender				
Male	78	45(81.8)	33 (84.6)	0.722
Female	16	10(19.2)	6(15.4)	
Grade				
I	13	7(12.5)	6(15.4)	0.687
II -III	82	49(87.5)	33(84.6)	
AFP (ng/mL)				
≤20	33	17(34.0)	15(39.5)	0.597
>20	56	33(66.0)	23(60.5)	
HBV				
Negative	27	21(38.2)	6(15.4)	0.016*
Positive	67	34(61.8)	33(84.6)	
Vessel carcinoma embolus (VCE)				
Negative	90	56(100.0)	34(84.6)	0.006**
Positive	5	0(0.0)	5(15.4)	
Intrahepatic Metastasis				
Negative	86	53(94.6)	33(67.7)	0.101
Positive	9	3 (5.4)	6 (32.3)	

AKR7A2 Promotes Oxidative Phosphorylation and Mitochondrial Biogenesis in HCC Cells

GSEA analysis showed that the AKR7A2 expression was positively correlated with genes related to "Electron transport chain" and "Oxidative phosphorylation" using TCGA data (Figure 3A-3D). Furthermore, the expression of key mediators of OXPHOS, including SDHB, UQCRC1, and ATP5A1 were positively correlated with AKR7A2 expression in HCC using TCGA data (Figure 4A).

Given that PPARG, TFAM, PGC1α, and c-Myc are well-established regulators of mitochondrial metabolism[23-25], we next investigated the correlation between AKR7A2 and these key regulatory genes. We found that expression of AKR7A2 was positively PPARG expression (Figure 4A). However, there is no significant positive correlation between the expression of AKR7A2 and the other three key genes (data not displayed). Therefore, these findings suggest that AKR7A2 may promote oxidative phosphorylation and mitochondrial biogenesis in HCC cells through the regulation of PPARG.

AKR7A2 Promotes HCC Progression by Affecting Tumor-Associated Macrophage Polarization

AKR7A2 expression is associated with the expression of M2 polarization-related genes (CD163 and IL-10) in HCC according to analysis of TCGA data (Figure 4B). Furthermore, we found that expression of AKR7A2 was positively correlated with M2 macrophage infiltration using GSE12368, GSE33731, and GSE10927 data (Figure 4C). In addition, expression of AKR7A2 was negatively correlated with M1 macrophage infiltration and $CD8^+$ T cell infiltration (Figure 4C). Therefore, these results suggest that AKR7A2 promotes HCC progression by affecting tumor-associated macrophage polarization.

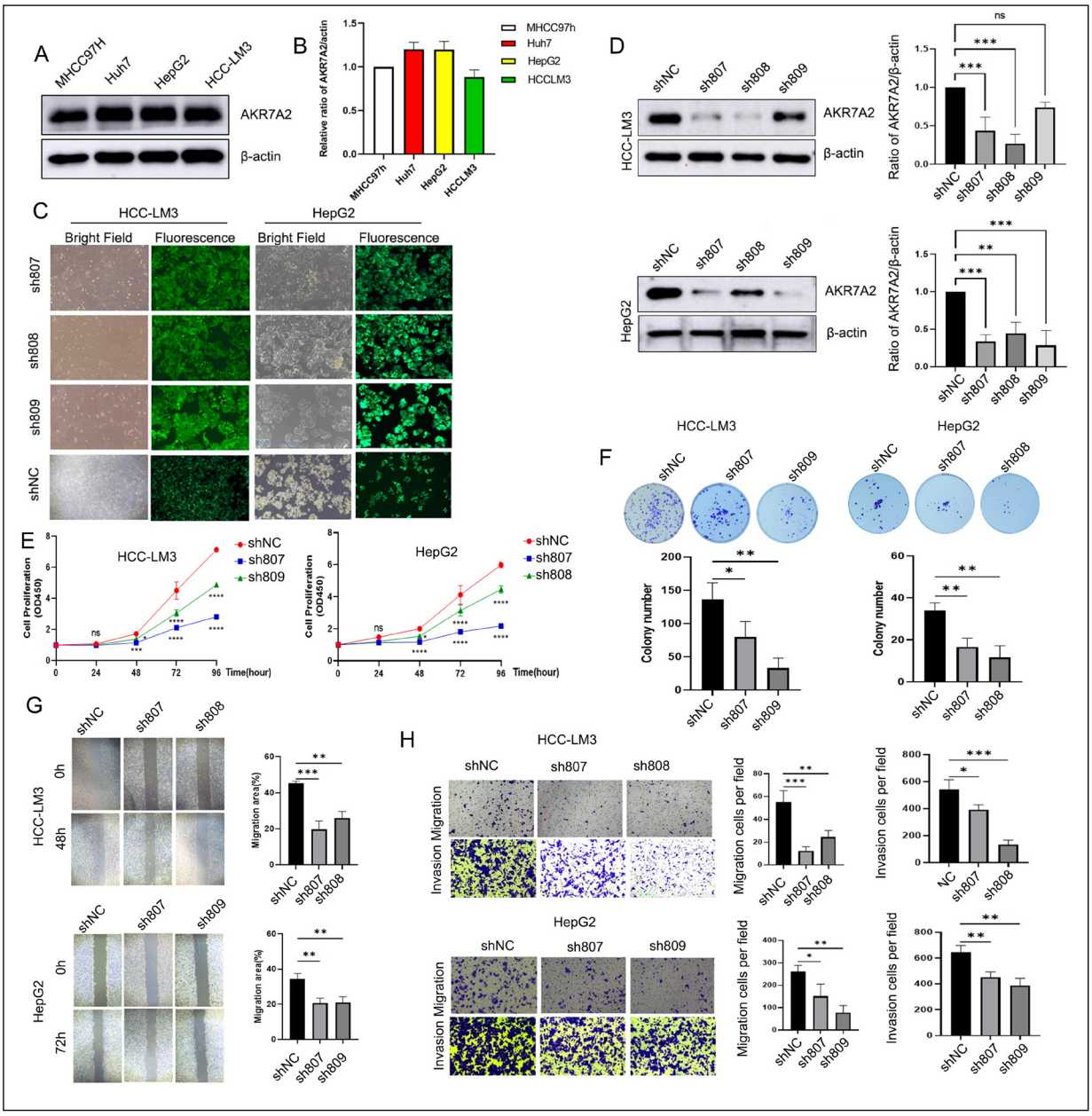

Figure 2. Knockdown of AKR7A2 inhibits HCC cell proliferation, migration, and invasion. *A-B*, The expression of AKR7A2 was detected by WB in HCC cells. *C*, Fluorescence image of knockdown AKR7A2 in HCC cells. *D*, AKR7A2 shRNA knockdown efficiency was validated using WB. *E*, Analysis of the effect of AKR7A2 knockdown on proliferation using CCK-8 assay. *F*, Analysis of the effect of AKR7A2 knockdown on proliferation using a colony formation assay. *G*, The effects of AKR7A2 knockdown on HCC cell migration were assessed by wound healing assay. *H*, The effects of AKR7A2 knockdown on HCC cell migration and invasion were assessed by Transwell assays.

DISCUSSION

AKR7A2 is a member of the AKR superfamily that utilizes NADP(H) as a cofactor to reduce aldehydes and ketones to their corresponding alcohols[26]. It is predominantly expressed in tissues such as the liver and kidney and exhibits catalytic activity toward aldehydes generated by lipid peroxidation, thereby contributing to the cellular defense against ROS and mitigating oxidative stress[27,15]. Notably, AKR7A2 is identical to human central nervous system succinic semialdehyde reductase (SSAR), an enzyme involved

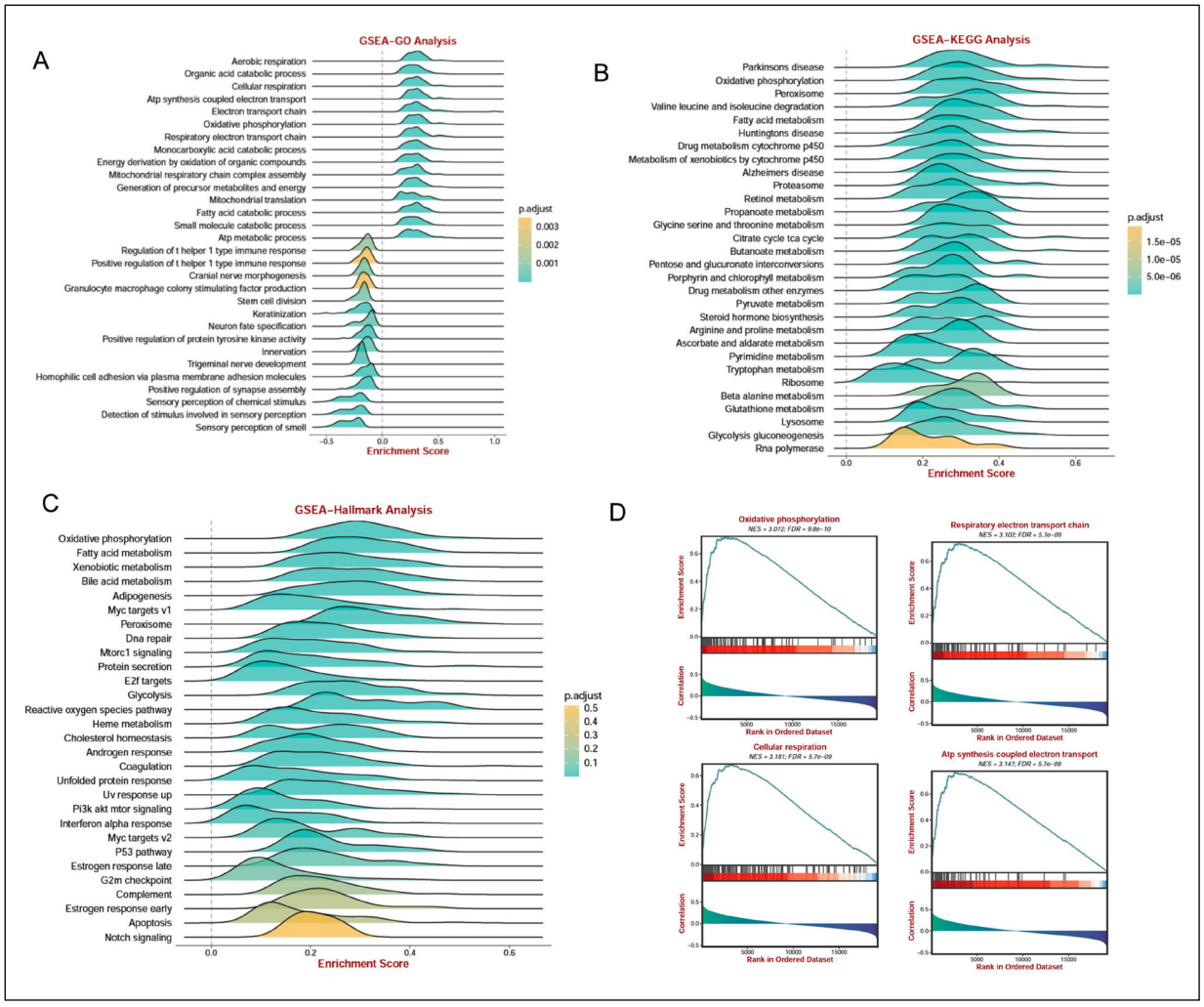

Figure 3. AKR7A2 promotes mitochondrial respiration and oxidative phosphorylation. GESA-GO analysis (*A*), GESA-KEGG analysis (*B*), and GESA-Hallmark analysis (C) were performed using TCGA data. D, GES analysis showed oxidative phosphorylation, respiratory electron transport chain, cellular respiration, ATP synthesis coupled electron transport.

in γ-aminobutyric acid (GABA) metabolism[28]. GABA directly binds to β-catenin and stabilizes it, leading to activation of the Wnt/β-catenin signaling pathway and promoting HCC metastasis[29]. In this study, we found that upregulated AKR7A2 was associated with poor prognosis of HCC. AKR7A2 increased HCC cell proliferation, migration, and invasion. Therefore, we speculated that the function of AKR7A2 may be related to its metabolic enzyme activity.

Metabolic reprogramming has been well-known as a hallmark of cancer[30]. Mitochondria are the main suppliers of energy and are responsible for the balance between glycolysis and OXPHOS. A growing number of studies showed that mitochondrial OXPHOS may be a significant metabolic pattern during metastasis[31,32]. Increased OXPHOS in cancer not only provides energy for dissemination but also enhances crosstalk in the tumor microenvironment[33]. In this study, we found that AKR7A2 expression was associated with OXPHOS and the electron transport chain (ETC) activity. Furthermore, we found a positive correlation between AKR7A2 and PPARG in HCC. Therefore, we speculated that AKR7A2 promoted OXPHOS and electron transport chain activity through PPARG.

Macrophages are the most abundant innate immune cells in the tumor microenvironment (TME)[34]. Tumor-associated macrophages (TAMs), which typically exhibit an M2-like polarization state, are key components of the TME and promote cancer metastasis through direct and indirect interactions with tumor cells[35]. M2-polarized macrophages secrete a range of immunosuppressive cytokines, growth factors, and extracellular mediators that collectively foster an immunosuppressive TME[36]. Immunoregulatory molecules, such as IL-10, contribute to M2 polarization[37], and TAMs further suppress anti-tumor immunity by expressing immune checkpoint molecules, including PD-L1[38]. A previous study showed

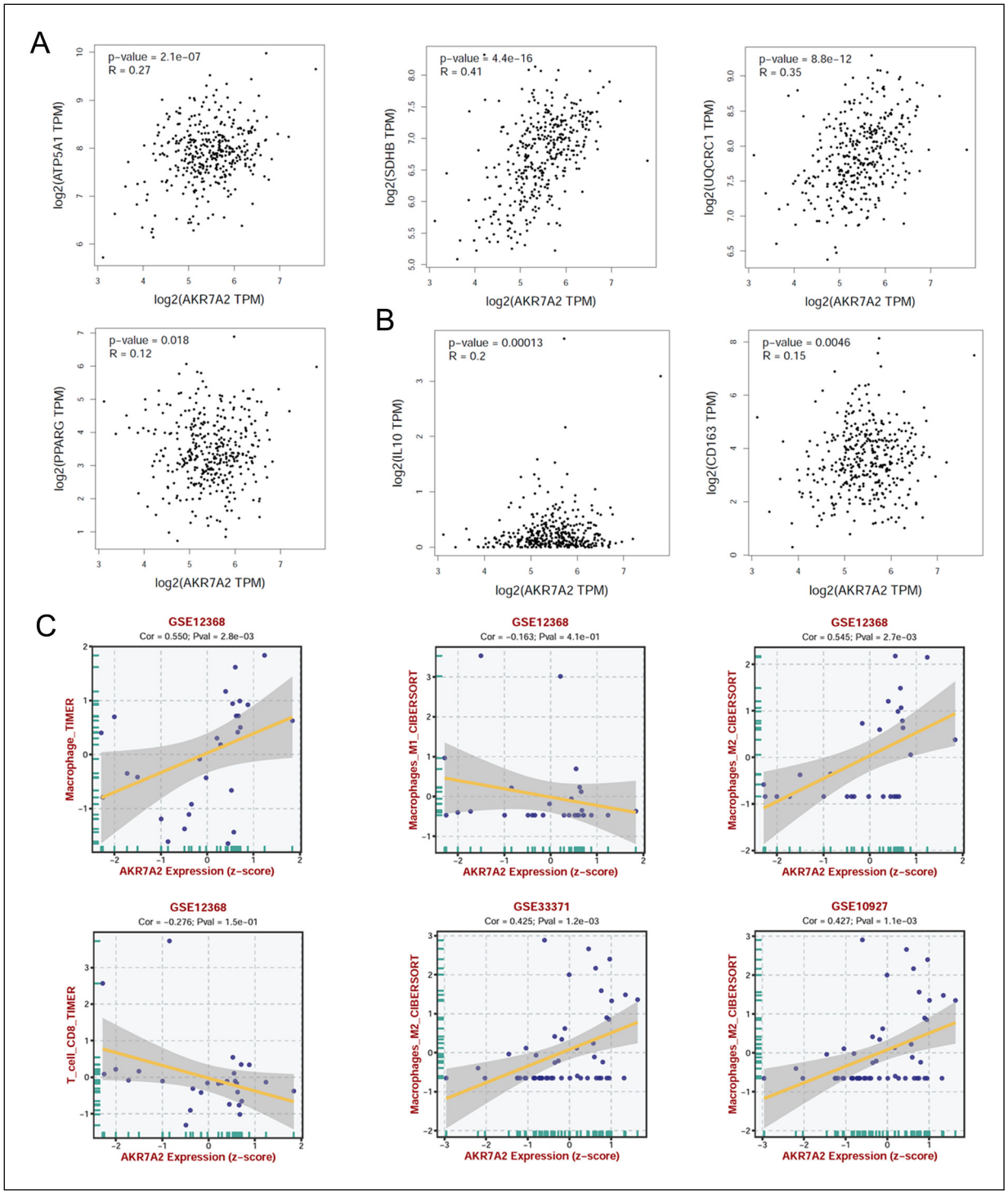

Figure 4. AKR7A2 expression associates with tumor-associated macrophage polarization. *A*, Expression of AKR7A2 was associated with ATP51A, SDHB, UQCRC1, and PPARG in HCC using TCGA data. *B*, Expression of AKR7A2 was associated with IL-10 and CD163 in HCC using TCGA data. *C*, Expression of AKR7A2 was associated with tumor-associated macrophage M2 polarization in HCC.

that M2 TAMs promoted HCC progression[39]. In this study, we found that AKR7A2 expression was positively associated with M2 macrophage infiltration in HCC tissues. Furthermore, a significant correlation was observed between AKR7A2 and key immunoregulatory markers, including IL-10 and CD163. These findings suggest that AKR7A2 may contribute to the establishment of an immunosuppressive tumor microenvironment by modulating the recruitment or polarization of M2 macrophages. However, the underlying molecular mechanisms require further investigation to be fully elucidated.

CONCLUSIONS

In conclusion, our findings demonstrated that AKR7A2 is upregulated in HCC and is associated with poor patient prognosis. AKR7A2 promotes HCC cell proliferation, migration, and invasion, potentially through enhancing OXPHOS and facilitating M2 macrophage infiltration. Our study elucidates a critical role for AKR7A2 in HCC progression and highlights its potential as a prognostic biomarker and therapeutic target.

Conflict of Interest:

The authors declare that they have no competing interests.

Funding:

This study was supported in part by grants from Guangxi Natural Science Foundation (2024GXNSFAA010061, 2025GXNSFAA069112).

Authors' Contributions:

Huan Cui (ORCID: https://orcid.org/0009-0007-1469-3767), Qinqin Long (ORCID: https://orcid.org/0000-0001-9891-1651), and Li Zhang (ORCID: https://orcid.org/0009-0004-9129-9032) conducted all experiments and analyzed the data. Hua Tian (ORCID: https://orcid.org/0000-0002-2316-1953) designed experiments, supervised the study, and wrote the main manuscript text. All authors have read and approved the final manuscript.

ORCID ID:

Huan Cui: 0009-0007-1469-3767
Qinqin Long: 0000-0001-9891-1651
Li Zhang: 0009-0004-9129-9032
Hua Tian: 0000-0002-2316-1953

Data Availability Statement:

The datasets generated during and/or analyzed during the current study are available from the corresponding author on reasonable request.

Ethics Approval:

The study was approved by the Ethics Committee of Affiliated Hospital of Youjiang Medical University for Nationalities (2024041901; 2024-03).

Informed Consent:

Informed consent was obtained from all patients before enrolment. All methods were performed according to relevant guidelines and regulations.

REFERENCES

1. Llovet JM, Kelley RK, Villanueva A, Singal AG, Pikarsky E, Roayaie S, Lencioni R, Koike K, Zucman-Rossi J, Finn RS. Hepatocellular carcinoma. Nat Rev Dis Primers 2021; 7: 6. Erratum in: Nat Rev Dis Primers 2024; 10: 10.
2. Ainiwaer A, Chen Y, Lu Y. Precise staging of advanced HCC promotes higher quality of personalized treatment management: Chinese experts consensus on precision diagnosis and management of advanced hepatocellular carcinoma (2023). Hepatoma Res 2024; 10: 4.
3. Wang LJ, Liu XL. Causal associations between inflammatory factors and liver cancer. World Cancer Research Journal 2023; 10: e2662.
4. Crouchet E, Almeida N, Durand SC, Parnot M, Oudot MA, Giannone F, Gadenne C, Roehlen N, Saviano A, Felli E, Pessaux P, Duong HT, Ohdan H, Aikata H, Chayama K, Baumert TF, Schuster C. A patient-derived HCC spheroid system to model the tumor microenvironment and treatment response. JHEP Rep 2024; 7: 101252.
5. Berardi G, Cucchetti A, Sposito C, Ratti F, Nebbia M, D'Souza DM, Pascual F, Dogeas E, Tohme S, Vitale A, D'Amico FE, Alessandris R, Panetta V, Simonelli I, Colasanti M, Russolillo N, Moro A, Fiorentini G, Serenari M, Rotellar F, Zimitti G, Famularo S, Ivanics T, Donando FG, Hoffman D, Onkendi E, Essaji Y, Giuliani T, Lopez Ben S, Caula C, Rompianesi G, Chopra A, Abu Hilal M, Sapisochin G, Torzilli G, Corvera C, Alseidi A, Helton S, Troisi RI, Simo K, Conrad C, Cescon M, Cleary S, Kwon DCH, Ferrero A, Ettorre GM, Cillo U, Geller D, Cherqui D, Serrano PE, Ferrone C, Aldrighetti L, Kingham TP, Mazzaferro V. Recurrence and tumor-related death after resection of hepatocellular carcinoma in patients with metabolic syndrome. JHEP Rep 2024; 6: 101075.

6. Tsakiridis EE, Ahmadi E, Gautam J, Hannah She YR, Fayyazi R, Lally JSV, Wang S, Di Pastena F, Valvano CM, Del Rosso D, Biziotis OD, Meyers B, Muti P, Tsakiridis T, Steinberg GR. Salsalate improves the anti-tumor efficacy of lenvatinib in MASH-driven hepatocellular carcinoma. JHEP Rep 2025; 7: 101354.
7. Montella L, Sarno F, Ambrosino A, Facchini S, D'Antò M, Laterza MM, Fasano M, Quarata E, Ranucci RAN, Altucci L, Berretta M, Facchini G. The Role of Immunotherapy in a Tolerogenic Environment: Current and Future Perspectives for Hepatocellular Carcinoma. Cells 2021; 10: 1909.
8. Nguyen LC, Luu DTM, Doan HTN, Nguyen NM, Nguyen HTT, Pham TT, Pham NB, Le TP, Nguyen TT, Nguyen HV. Prognostic factor and risk stratification in hepatocellular carcinoma: insights from Cox regression and Kaplan-Meier analysis in a male-dominated cohort. Eur Rev Med Pharmacol Sci 2024; 28: 4701-4711.
9. Fu C, Chen H, Chen Y, Liu W, Cao G. Transarterial intervention therapy combined with systemic therapy for HCC: a review of recent five-year articles. Hepatoma Research 2024; 10: 42.
10. Rao M, Chang KC. Aldose reductase is a potential therapeutic target for neurodegeneration. Chem Biol Interact 2024; 389: 110856.
11. Nagini S, Kallamadi PR, Tanagala KKK, Reddy GB. Aldo-keto reductases: Role in cancer development and theranostics. Oncol Res 2024; 32: 1287-1308.
12. Zhou Q, Tian W, Jiang Z, Huang T, Ge C, Liu T, Zhao F, Chen T, Cui Y, Li H, Yao M, Li J, Tian H. A Positive Feedback Loop of AKR1C3-Mediated Activation of NF-kappaB and STAT3 Facilitates Proliferation and Metastasis in Hepatocellular Carcinoma. Cancer Res 2021; 81: 1361-1374.
13. Chen J, Zhang J, Tian W, Ge C, Su Y, Li J, Tian H. AKR1C3 suppresses ferroptosis in hepatocellular carcinoma through regulation of YAP/SLC7A11 signaling pathway. Mol Carcinog 2023; 62: 833-844.
14. Li D, Chen J, Zhou F, Zhang W, Chen H. Aldo-keto reductase-7A2 protects against atorvastatin-induced hepatotoxicity via Nrf2 activation. Chem Biol Interact 2024; 393: 110956.
15. Li D, Ferrari M, Ellis EM. Human aldo-keto reductase AKR7A2 protects against the cytotoxicity and mutagenicity of reactive aldehydes and lowers intracellular reactive oxygen species in hamster V79-4 cells. Chem Biol Interact 2012; 195: 25-34.
16. Li X, Zou S, Li Z, Cai G, Chen B, Wang P, Dong W. The identification of human aldo-keto reductase AKR7A2 as a novel cytoglobin-binding partner. Cell Mol Biol Lett 2016; 21: 25.
17. Tian W, Yang Y, Meng L, Ge C, Liu Y, Zhang C, Huang Z, Zhang C, Tian H. GCDH Acetylation Orchestrates DNA Damage Response and Autophagy via Mitochondrial ROS to Suppress Hepatocellular Carcinoma Progression. Research (Wash D C) 2025; 8: 0862.
18. Zhang W, Tian W, Xia X, Tian H, Sun T. AKR1C3 protects cardiomyocytes against hypoxia-induced cell apoptosis through the Nrf-2/NF-kappaB pathway. Acta Biochim Biophys Sin (Shanghai) 2025; 57: 1151-1163.
19. Su Y, Meng L, Ge C, Liu Y, Zhang C, Yang Y, Tian W, Tian H. PSMD9 promotes the malignant progression of hepatocellular carcinoma by interacting with c-Cbl to activate EGFR signaling and recycling. J Exp Clin Cancer Res 2024; 43: 142.
20. Ganesan K, Xu C, Wu S, Sui Y, Du B, Zhang J, Gao F, Chen J, Tang H. Ononin Inhibits Tumor Bone Metastasis and Osteoclastogenesis By Targeting Mitogen-Activated Protein Kinase Pathway in Breast Cancer. Research (Wash D C) 2024; 7: 0553.
21. Zhou Q, Huang T, Jiang Z, Ge C, Chen X, Zhang L, Zhao F, Zhu M, Chen T, Cui Y, Li H, Yao M, Li J, Tian H. Upregulation of SNX5 predicts poor prognosis and promotes hepatocellular carcinoma progression by modulating the EGFR-ERK1/2 signaling pathway. Oncogene 2020; 39: 2140-2155.
22. Tian H, Ge C, Li H, Zhao F, Hou H, Chen T, Jiang G, Xie H, Cui Y, Yao M, Li J. Ribonucleotide reductase M2B inhibits cell migration and spreading by early growth response protein 1-mediated phosphatase and tensin homolog/Akt1 pathway in hepatocellular carcinoma. Hepatology 2014; 59: 1459-1470.
23. Piccinin E, Arconzo M, Matrella ML, Cariello M, Polizzi A, Lippi Y, Bertrand-Michel J, Guillou H, Loiseau N, Villani G, Moschetta A. Intestinal Pgc1alpha ablation protects from liver steatosis and fibrosis. JHEP Rep 2023; 5: 100853.
24. Zheng Q, Tang J, Aicher A, Bou Kheir T, Sabanovic B, Ananthanarayanan P, Reina C, Chen M, Gu JM, He B, Alcala S, Behrens D, Lawlo RT, Scarpa A, Hidalgo M, Sainz B, Jr., Sancho P, Heeschen C. Inhibiting NR5A2 targets stemness in pancreatic cancer by disrupting SOX2/MYC signaling and restoring chemosensitivity. J Exp Clin Cancer Res 2023; 42: 323.
25. LeBleu VS, O'Connell JT, Gonzalez Herrera KN, Wikman H, Pantel K, Haigis MC, de Carvalho FM, Damascena A, Domingos Chinen LT, Rocha RM, Asara JM, Kalluri R. PGC-1α mediates mitochondrial biogenesis and oxidative phosphorylation in cancer cells to promote metastasis. Nat Cell Biol 2014; 16: 992-1003, 1-15. Erratum in: Nat Cell Biol 2014; 16: 1125.
26. Barski OA, Tipparaju SM, Bhatnagar A. The aldo-keto reductase superfamily and its role in drug metabolism and detoxification. Drug Metab Rev 2008; 40: 553-624.
27. O'Connor T, Ireland LS, Harrison DJ, Hayes JD. Major differences exist in the function and tissue-specific expression of human aflatoxin B1 aldehyde reductase and the principal human aldo-keto reductase AKR1 family members. Biochem J 1999; 343 Pt 2: 487-504.
28. Schaller M, Schaffhauser M, Sans N, Wermuth B. Cloning and expression of succinic semialdehyde reductase from human brain. Identity with aflatoxin B1 aldehyde reductase. Eur J Biochem 1999; 265: 1056-1060.
29. Li L, Kang Y, Cheng R, Liu F, Wu F, Liu Z, Kou J, Zhang Z, Li W, Zhao H, He X, Du W. The de novo synthesis of GABA and its gene regulatory function control hepatocellular carcinoma metastasis. Dev Cell 2025; 60: 1053-69e6.
30. Mir R, Javid J, Ullah MF, Alrdahe S, Altedlawi IA, Mustafa SK, Jalal MM, Altayar MA, Albalawi AD, Abunab MK, Alanazi HS, Barnawi J, Algehainy NA, Altemani FH, Tayeb FJ. Metabolic reprogramming and functional crosstalk within the tumor microenvironment (TME) and A Multi-omics anticancer approach. Med Oncol 2025; 42: 373.
31. Li SS, Zhang B, Huang C, Fu Y, Zhao Y, Gong L, Tan Y, Wang H, Chen W, Luo J, Zhang Y, Ma S, Fu L, Liu C, Huang J, Ju HQ, Lee AW, Guan XY. FAO-fueled OXPHOS and NRF2-mediated stress resilience in MICs drive lymph node metastasis. Proc Natl Acad Sci U S A 2025; 122: e2411241122
32. Liu Y, Tian W, Ge C, Zhang C, Huang Z, Zhang C, Yang Y, Tian H. SNX17 mediates STAT3 activation to promote hepatocellular carcinoma progression via a retromer dependent mechanism. Int J Biol Sci 2025; 21: 2762-2779.
33. Wang R, Zhuang J, Zhang Q, Wu W, Yu X, Zhang H, Xie Z. Decoding the metabolic dialogue in the tumor microenvironment: from immune suppression to precision cancer therapies. Exp Hematol Oncol 2025; 14: 99.
34. Cheng K, Cai N, Zhu J, Yang X, Liang H, Zhang W. Tumor-associated macrophages in liver cancer: From mechanisms to therapy. Cancer Commun (Lond) 2022; 42: 1112-1140.

35. Liu L, Li Y, Li B. Interactions between cancer cells and tumor-associated macrophages in tumor microenvironment. Biochim Biophys Acta Rev Cancer 2025; 1880: 189344.
36. Han S, Bao X, Zou Y, Wang L, Li Y, Yang L, Liao A, Zhang X, Jiang X, Liang D, Dai Y, Zheng QC, Yu Z, Guo J. d-lactate modulates M2 tumor-associated macrophages and remodels immunosuppressive tumor microenvironment for hepatocellular carcinoma. Sci Adv 2023; 9: eadg2697.
37. Zhong CR, Wu ZF, Zheng ZQ, Lin Z, Liang YL, Lin ZJ, Wan YL, Li GL. Radiotherapy-induced TACC3 confers resistance of HCC to radiotherapy and enhances IL4-dependent immunosuppression to exacerbate hepatocarcinogenesis. Cancer Lett 2025; 627: 217819.
38. Luo F, Mei Y, Li Y, Yang J, Xi S, Cao E, Shen C, Zhou D, Wang P, Zhou D, Cai H. CAF-derived LRRC15 orchestrates macrophage polarization and limits PD-1 immunotherapy efficacy in glioblastoma. Neuro Oncol 2025: noaf157. Epub ahead of print.
39. Li J, Zhang C, Zhou Q, Long Q, Chen J, Meng L, Tian W, Yang Y, Ge C, Su Y, Long XD, Wu J, Tian H. ALDH1L2 drives HCC progression through TAM polarization. JHEP Rep 2025; 7: 101217.